Environmental Science and Pollution Research (2019) 26:11535–11541
https://doi.org/10.1007/s11356-018-1497-1

LOW COST ORGANIC AND INORGANIC SORBENTS TO FIGHT SOIL AND WATER POLLUTION

Comparative study of calcium alginate, ball-milled biochar, and their composites on aqueous methylene blue adsorption

Bing Wang [1,2,3] · Bin Gao [2] · Yongshan Wan [4]

Received: 15 November 2017 / Accepted: 5 February 2018 / Published online: 20 February 2018

Abstract

In this work, a novel composite, ball-milled biochar (BMB) encapsulated in calcium-alginate (CA) beads (CA-BMB), was synthesized as an alternative adsorbent for the removal of methylene blue (MB) from an aqueous solution. Sorption performance was compared among CA, BMB, and CA-BMB composite with batch adsorption experiments. With 25% BMB and 75% alginate, the new composite resembled CA in MB adsorption. With an initial MB concentration of 50 mg L^{-1}, kinetics studies showed that 74% MB removal by CA-BMB was achieved within 8 h, followed by slow kinetics reaching 91% removal in 16 h. The adsorption kinetics was well explained by the Ritchie's kinetic model, indicative of energetically heterogeneous solid surface of the composite. Adsorption isotherms of BMB, CA, and CA-BMB can all be fitted with the Langmuir models; the adsorption capacity of CA-BMB (1210.7 mg g^{-1}) was close to that of CA (1282.2 mg g^{-1}) and much higher than that of BMB alone (184.1 mg g^{-1}). The outstanding adsorption performance suggested that CA-BMB can serve as a low-cost and eco-friendly adsorbent for MB removal from an aqueous solution.

Keywords Ball mill · Biochar · Sodium alginate · Methylene blue · Wastewater · Adsorption

Introduction

Environmental and health concerns of wastewater containing methylene blue (MB), a cationic dye heavily used in dyeing and textile industries, challenge scientists and engineers to search for low-cost, eco-friendly adsorbent materials as alternatives of conventional activated carbon, which is expensive for the removal of dyes from industrial effluents (Ding et al. 2016; Yagub et al. 2014; Zhang and Gao 2013). Novel engineered materials such as carbon nanotubes, biochar, and graphene have been reported to possess excellent abilities for adsorption of pollutants including MB (Fang et al. 2016; Gupta et al. 2013). In terms of cost-effectiveness, biochar perhaps draws the most attention, partly due to the fact that most feedstock materials for biochar production are waste biomass and readily available (Inyang et al. 2016; Xu et al. 2017). However, newly prepared, pristine biochar generally has lower adsorption capacity than activated carbon (Fang et al. 2016). Thus, functionalizing pristine biochar to improve its adsorption performance has become an important area of research for expanding the environmental applications of biochar technology (Ahmad et al. 2014; Rajapaksha et al. 2016; Wang et al. 2017). A few workers noted that ball milling can greatly improve the adsorption capacity of biochar by increasing its surface area (Lyu et al. 2017, 2018a, b; Peterson et al. 2012). However, ball-milled biochar (BMB) is nanosized, and its mobility with water is of potential environmental and human health concern if not stabilized in a matrix material (Helland et al. 2008; Hoet et al. 2004; Lam et al. 2006).

Responsible editor: Philippe Garrigues

✉ Bin Gao
bg55@ufl.edu

[1] State Key Laboratory of Environmental Geochemistry, Institute of Geochemistry, Chinese Academy of Sciences, Guiyang 550081, China

[2] Department of Agricultural and Biological Engineering, University of Florida, Gainesville, FL 32611, USA

[3] Puding Karst Ecosystem Research Station, State Key Laboratory of Environmental Geochemistry, Institute of Geochemistry, Chinese Academy of Sciences, Puding 562100, China

[4] National Health and Environmental Effects Research Laboratory, US EPA, Gulf Breeze, FL 32561, USA

Alginate, which is commercially available salt of alginic acid extracted from brown seaweeds, has drawn much attention in biomedical applications (Lee and Mooney 2012) and environmental remediation such as removal of heavy metals and dyes from aqueous solutions (Mahmoodi 2011; Park et al. 2006). As a natural polymer, alginate is rich in carboxylate functional groups. It possesses a special functionality in thickening aqueous solutions and forming gels when divalent cations (such as Ca^{2+}) are present in a solution. Thus, a unique environmental application of alginate is to encapsulate other adsorbents such as chitosan, graphene oxide, epichlorohydrin, activated carbon, and carbon nanotubes to enhance their adsorption performance (Ai et al. 2011; Gong et al. 2009; Gotoh et al. 2004; Kulkarni et al. 2000; Li et al. 2013; Lin et al. 2005; Liu et al. 2012; Rocher et al. 2010).

In this study, we hypothesize that calcium alginate (CA) can help stabilize ball-milled biochar, thereby creating a new composite (CA-BMB) which may improve dye adsorption capacity of BMB. Specifically, the objectives of the study are to (1) compare the MB sorption performance among BMB, CA, and CA-BMB composite; (2) study MB adsorption kinetics and thermodynamic equilibrium; and (3) evaluate the application potential of BMB after encapsulated in Ca-alginate.

Methods and experiments

Chemicals and reagents

Sodium alginate, methylene blue (MB), calcium chloride ($CaCl_2$), and sodium hydroxide (NaOH) were purchased from Fisher Scientific. All the chemicals and reagents used in this study were of reagent grade (GR grade) and used without any further purification.

Preparation of the ball-milled biochar

Biochar used in this study originated from bamboo feedstock.The raw materials were oven dried (80 °C) and converted into biochar through slow pyrolysis using a furnace (Olympic 1823HE) in a N_2 environment at temperatures of 450 °C. The biochar was mechanically activated in a planetary ball mill (Across International, PQ-N_2) in an air atmosphere, at room temperature using 500 mL capacity agate milling jars and lids. The milling media consisted of an agate vial with 5 × 20 and 10 × 10 mm agate balls. In all milling runs, the ball-to-powder weight ratio was 100:1 and the rotational speed of the main disk was 300 rpm. In each run, the biochar was milled for a total of 12 h (four 3-h shifts in opposite directions with a 10-min rest period in between). After milling, samples were collected and saved for use.

Preparation of beads

The ball-milled biochar (BMB) was dispersed in a liquid state of Na-alginate (1% *w*/*v*) from macrosyticapyrifera, high viscosity (MP Biomedicals, Inc. Co., USA) at the mass ratio of 25% BMB and 75% alginate. This ratio was used as an example to test the hypothesie that CA can help stabilize BMB. In addition, alginate was more than enough to hold the BMB at the ratio. An ultrasound was then applied using a Model B3510-MT Ultrasonic Cleaner (Branson Ultrasonics Co., USA, with a nominal frequency of 40 kHz) for 2 h at 25 °C to get a uniform dispersion of the sodium alginate-BMB aqueous solution. 0.1 M $CaCl_2$ solution was used to form Ca-alginate and Ca-alginate-BMB beads. The Ca-alginate beads were obtained by dropwise addition of 100 mL sodium alginate-BMB solution into 500 mL 0.1 M $CaCl_2$ solution using a 60-mL syringe fitted with 23G1 Precision Glide needles (BD) to form CA-BMB beads. Ca-alginate-BMB beads were left overnight to stabilize. The beads were washed several times with deionized water to remove residual BMB particles and non-cross-linked calcium ions from the surface of the beads. Pure CA beads were prepared similarly. The diameters of both beads were approximately 2.03 ± 0.04 mm.

Characterizations of adsorbents

The adsorbents were characterized using scanning electron microscope (SEM) analysis to illustrate their morphology. The samples were imaged with a beam energy of 20 kV on a JSM-6460LV SEM. The specific surface area and pore size distributions of the adsorbents were measured by N_2 sorptometry on a Quantachrome Autosorb I, at 77 K. Samples were degassed under vacuum for least 24 h at 180 °C prior to analysis. Surface area was calculated according to BET theory using adsorption data in the 0.01–0.3 relative pressure range.

MB adsorption experiments

Stock solutions of MB (1000 mg L^{-1}) were prepared by dissolving MB volumetrically in deionized water. All batch adsorption experiments were conducted on a New Brunswick rotary shaker at 150 rpm with triplicate at room temperature. To determine the effect of initial pH on MB sorption, 0.1 M HNO_3 or 0.1 M NaOH was used to adjust the pH of 50 mg L^{-1} MB solutions to 3, 5, 7, 9, and 11. The batch experiment was initiated by mixing 0.010 g of the sorbent with 40 mL of MB solutions in 50 mL centrifuge tubes (Fisher Scientific). After shaking for 24 h, samples were filtered using a 0.22-μm syringe filter (PVDF syringe filter; Whatman). Concentrations of MB in the solution were measured using a GENESYS 10S UV-Vis spectrophotometer at 665 nm (Thermo Fisher Scientific).

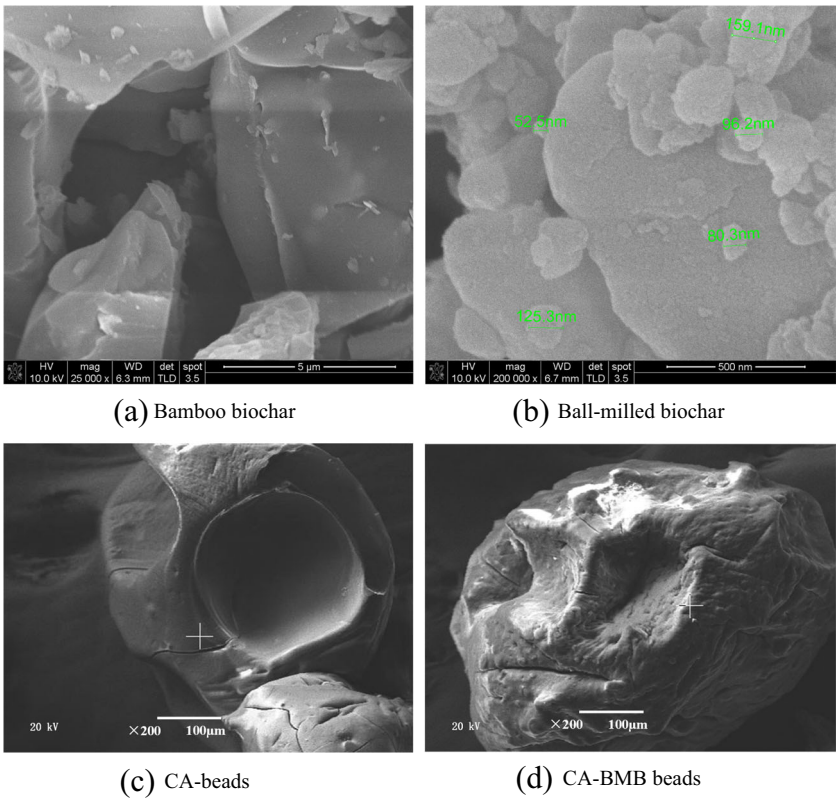

Fig. 1 The scanning electron micrographs (SEMs) of **a** bamboo biochar, **b** ball-milled biochar, **c** CA beads, and **d** CA-BMB beads

Sorption kinetics were examined by mixing 0.010 g of the adsorbent with 40 mL of 50 mg L^{-1} MB solutions in 50-mL centrifuge tubes (Fisher Scientific). The tubes were shaken on the New Brunswick shaker at time intervals of 0.083, 0.5, 1, 2, 4, 8, 16, and 24 h, and MB concentrations were measured. Sorption isotherms were constructed by mixing 0.010 g of each adsorbent with 40 mL of the MB solution of varying concentrations (30–800 mg L^{-1}). The suspension was shaken for 24 h and MB concentrations analyzed as described previously. All the sorption experiments were conducted in triplicate at fixed pH 5.0, and the average experimental data were reported. Various models were used to simulate the sorption kinetics and isotherms.

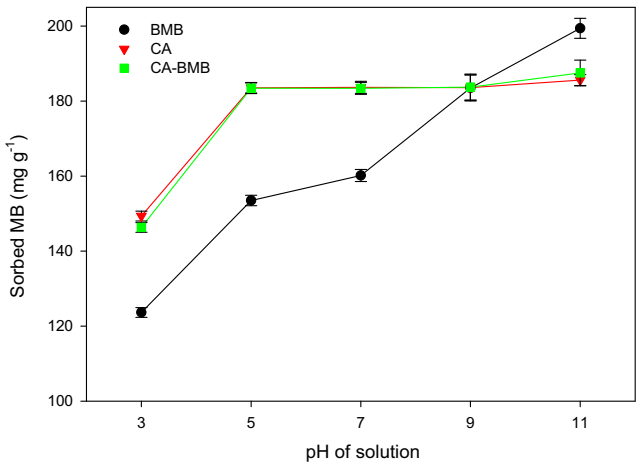

Fig. 2 The MB sorption capacity of CA, BMB, and CA-BMB at different pH conditions, pH = 3.07, 4.95, 6.97, 9.00, and 10.97. Symbols may cover error bars. Initial MB concentration 50 mg L^{-1}, contact time 24 h, temperature 298 K, adsorbent dose 250 mg L^{-1}, MB solution 40 mL

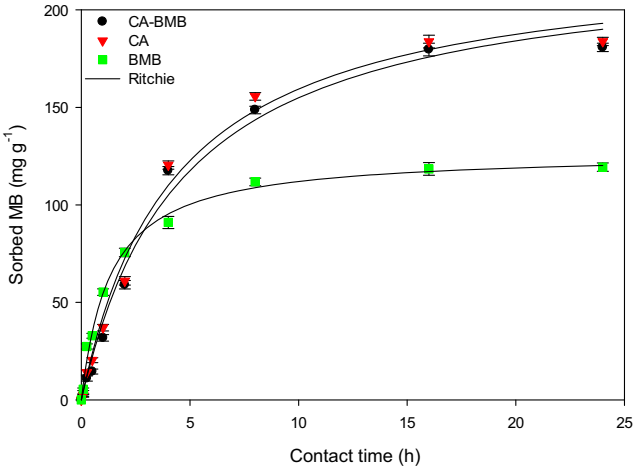

Fig. 3 The effect of contact time on the removal of MB by BMB, CA, and CA-BMB. Error bars represent standard error of triplicate samples ($n = 3$). Symbols may cover error bars. Initial MB concentration 50 mg L^{-1}, temperature 298 K, adsorbent dose 250 mg L^{-1}, MB solution 40 mL

Table 1 Summary best-fit parameters of various kinetic models for MB sorption onto CA, BMB, and CA-BMB

Sorbent	Model	Parameter 1	Parameter 2	R^2
CA	Pseudo-first order	$k_1 = 0.232$	$q_e = 186.5$	0.997
	Pseudo-second order	$k_2 = 0.00103$	$q_e = 227.5$	0.991
	Elovich	$\alpha = 71.5$	$\beta = 0.0169$	0.978
	Ritchie	$k_n = 0.0000735$	$q_e = 187.0$	0.997
BMB	Pseudo-first order	$k_1 = 0.584$	$q_e = 114.2$	0.980
	Pseudo-second order	$k_2 = 0.00598$	$q_e = 126.8$	0.995
	Elovich	$\alpha = 202.3$	$\beta = 0.041$	0.982
	Ritchie	$k_n = 0.00174$	$q_e = 133.8$	0.996
CA-BMB	Pseudo-first order	$k_1 = 0.219$	$q_e = 183.9$	0.996
	Pseudo-second order	$k_2 = 0.000949$	$q_e = 226.9$	0.990
	Elovich	$\alpha = 63.1$	$\beta = 0.0165$	0.977
	Ritchie	$k_n = 0.0000603$	$q_e = 184.3$	0.996

Results and discussion

Characterizations

The specific surface area is 18.2 $m^2\ g^{-1}$ for the original bamboo biochar and 298.6 $m^2\ g^{-1}$ for the BMB (Lyu et al. 2018a, b), showing a 16-time increase in specific surface area with ball milling. The scanning electron micrographs (SEMs) of bamboo biochar exhibited smooth surface while that of BMB indicated nanosized biochar particles after ball billing (Fig. 1), supporting the increased specific surface area of BMB. The SEM of the CA-BMB bead showed rougher surface than the CA bead, indicative of nanosized BMB in the CA-BMb bead (Fig. 1).

pH effect on the MB adsorption

Solution pH influences the surface charge, the degree of ionization, and the extent of dissociation of the functional groups on the active sites of the adsorbent (Gupta et al. 2004; Wang et al. 2005). Under acidic conditions, functional groups in BMB, CA, or CA-BMB adsorb H^+, producing electrostatic repulsion of cationic MB (positively charged). As the initial solution pH increased from 3 to 11, a nearly linear increase in MB adsorption was observed for BMB (from 122 to 200 mg g^{-1}, Fig. 2), indicative of deprotonation of functional groups (e.g., carboxyl). However, the increase in MB adsorption for CA and CA-BMB plateaued at about 185 mg^{-1} g after pH reached five (Fig. 2).

MB adsorption kinetics

Figure 3 shows MB adsorption kinetics of BMB, CA, and CA-BMB with 50 mg L^{-1} initial concentrations. The MB uptake by BMB was relatively fast with more than 80% of the adsorption completed within 4 h. However, the MB sorption by CA and CA-BMB exhibited an initial rapid uptake, removing 78 and 74% of the MB within 8 h, followed by slow kinetics that reached a plateau in 16 h whereby MB removal was about 91%. The initial rapid update is indicative of external mass transfer to occupy high-affinity binding sites while the slow kinetics involves occupying residual low-affinity binding sites. This two-stage process resulted in a longer equilibrium time than most MB sorbents reported in the literature (Bulut and Aydın 2006; Doğan et al. 2004).

Sorption kinetics modeling of the experimental data may provide additional insight on potential rate-controlling steps and mechanisms in the sorption process (Li et al. 2005). In this study, pseudo-first-order, pseudo-second-order, Elovich, and Ritchie models were used to simulate the sorption kinetics data:

$$q_t = q_e\left(1-e^{-k_1 t}\right), \text{pseudo-first order} \quad (1)$$

$$q_t = \frac{k_2 {q_e}^2 t}{1 + k_2 q_e t}, \text{pseudo-second order} \quad (2)$$

$$q_t = \frac{1}{\beta}\ln(\alpha\beta t + 1), \text{Elovich} \quad (3)$$

$$q_t = q_e - \left(q_e^{1-n}\frac{k_n}{1-n}t\right)^{\frac{1}{1-n}}, \text{Ritchie} \quad (4)$$

where q_t (mg g^{-1}) and q_e (mg g^{-1}) are the amounts of MB sorbed at time t and at equilibrium, respectively; k_1 (h^{-1}), k_2 (g mg^{-1} h^{-1}), and k_n (g^{n-1} mg^{1-n} h^{-1}) are the first-order, second-order, and Ritchie nth-order sorption rate constants. α (mg g^{-1} h^{-1}) is the initial sorption rate, and β (g mg^{-1}) is the desorption constant.

Usually, the pseudo-first-order kinetics is applied to the process of pure physical adsorption. The pseudo-second-order kinetics is based on the assumption that the rate-limiting step is chemical adsorption or physicochemical adsorption involving the transfer, exchange, and co-occurrence of electrons. The Elovich equation describes chemical adsorption processes and is often used for adsorbents with

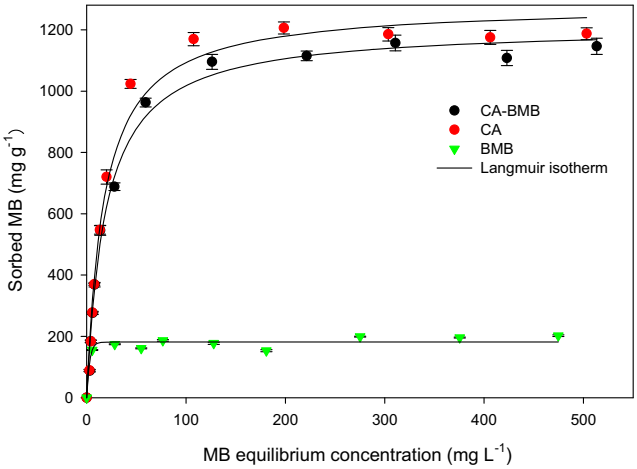

Fig. 4 MB adsorption isotherms of CA, BMB, and CA-BMB. Error bars represent standard error of triplicate samples ($n = 3$). Symbols may cover error bars. Contact time 24 h, temperature 298 K, adsorbent dose 250 mg L^{-1}, MB solution 40 mL

heterogeneous surfaces. Ritchie's kinetics describes adsorption on energetically heterogeneous solid surfaces. Table 1 shows the best-fit parameters of these kinetic models. In general, Ritchie's kinetics model provided the best fit of the experimental data for all three adsorbents through the pseudo-first-order model was as good for CA and CA-BMB and the pseudo-second-order model was almost as good for BMB, implying that MB adsorption kinetics by CA or CA-BMB was mostly through physical sorption on energetically heterogeneous solid surfaces.

MB adsorption isotherms

Several mathematical models have been used to describe adsorption equilibrium (Foo and Hameed 2010; Limousin et al. 2007), and the most frequently used ones are the Langmuir and Freundlich models:

$$\text{Langmuir isotherm}: q_e = Q_o k_L C_e/(1 + k_L C_e) \quad (5)$$

$$\text{Freundlich isotherm}: q_e = k_f C_e^{1/n} \quad (6)$$

where q_e (mg MB g^{-1}) is the adsorption capacity; C_e (mg MB L^{-1}) is the equilibrium concentration after the adsorption or desorption; $1/n$ (dimensionless) is the intensity of adsorption or affinity; k_f ($mg^{1-1/n}$ $L^{1/n}$ g^{-1}) is the Freundlich adsorption constant; Q_o (mg MB g^{-1}) is the maximum sorption capacity; k_L (L mg^{-1}) is a Langmuir constant.

Table 2 Fitted parameter values using different adsorption isotherm models

Adsorbent	Langmuir adsorption model			Freundlich adsorption model		
	Q_o (mg MB g^{-1})	k_L	R^2	k_f	$1/n$	R^2
CA	1282.2	0.058	0.986	266.7	3.803	0.861
BMB	184.1	0.854	0.935	139.0	18.5	0.953
CA-BMB	1210.7	0.053	0.993	239.7	3.692	0.893

Contact time 24 h, temperature 298 K, adsorbent dose 250 mg L^{-1}, MB solution 40 mL

Table 3 Previously reported adsorption capacities of MB onto various sorbents

Adsorbent	Q_0 (mg MB g^{-1})	Ref.
Activated carbon	454.2	Hameed et al. (2007)
Carbon nanotubes	35.4–64.7	Yao et al. (2010)
M-MWCNTs	48.06	Ai et al. (2011)
Alg-HNT hybrid beads	222	Liu et al. (2012)
Ca-alginate/AC beads	892	Hassan et al. (2014)
GO/Ca-alginate composites	181.81	Li et al. (2013)
Montmorillonite clay	289.12	Almeida et al. (2009)
MWCNTs	103.6	Zohre et al. (2010)
Ca-alginate bentonite AC beads	994.06	Benhouria et al. (2015)
Calcium alginate beads	800	Hassan et al. (2014)
Agar@BMNPs	875	Patra et al. (2016)
ASL	769	Manna et al. (2017)
Platanus orientalis leaves powder	114	Peydayesh and Rahbar-Kelishami (2015)
Ca-alginate-BMB	1210.7	This study

AB-alginate beads activated carbon-bentonite-alginate beads, *M-MWCNT* magnetic magnetite (Fe_3O_4)-loaded multiwall carbon nanotubes, *Alg-HNT hybrid beads* alginate-halloysite nanotube hybrid beads, *GO/Ca-alginate composites* graphene oxide/Ca-alginate composites, *Agar@BMNPs* monometallic/bimetallic nanoparticles incorporated agar, *ASL* alkali-steam treated lignocellulosic

The experimental data (Fig. 4) were used to derived parameters of these two equations using non-linear regression. Fitted parameter values of these adsorption isotherm models are given in Table 2. The equilibrium MB adsorption isotherms of CA, BMB, and CA-BMB can be best described by the Langmuir equation. The calculated adsorption capacities of CA, BMB, and CA-BMB were 1282.2, 184.1, and 1210.7 mg g^{-1}, respectively, manifesting significant improvement in MB adsorption of BMB after cross-linked with CA. The excellent fit with Langmuir equation may also suggest that MB adsorption is monomolecular adsorption that it is likely achieved through the Donnan membrane effects between CA and BMB (Sarkar et al. 2010).

Compared with other adsorbents including Ca-alginate/activated carbon beads and Ca-alginate beads previously reported by Hassan et al. (2014), the CA-BMB composite in this study exhibited superior MB adsorption capacity (Table 3). With 25% low-cost biochar and 75% alginate, the CA-BMB composite can be utilized as an inexpensive, highly effective adsorbent for the removal of MB from an aqueous solution.

Conclusions

It is now demonstrated that nanosized ball-milled biochar can be effectively stabilized in calcium alginate beads to produce a novel adsorbent for the removal of methylene blue from an aqueous solution. The new composite material contains 25% ball-milled biochar and 75% alginate. The equilibrium adsorption data are well fitted by the Langmuir isotherm, exhibiting a methylene blue adsorption capacity as high as 1210.7 mg g^{-1}. The adsorption kinetics can be best described with Richie's kinetics model, indicative of energetically heterogeneous solid surface of the composite. The optimal pH ranges from 5 to 11. The new material may serve as a cost-effective, eco-friendly adsorbent for the removal of methylene blue from an aqueous solution.

Funding information This work was financially supported by the National Key Research and Development Program of China (2016YFC0502602), the National Science Foundation of China (U1612441), the Key Agriculture R & D Program of Guizhou Province (NZ [2013]3012), the International Scientific and Technological Cooperation Project of Guizhou Province (G[2012]7050), the "Dawn of West China" Talent Training Program of the Chinese Academy of Sciences (grant number [2012]179), and the Opening Fund of State Key Laboratory of Environmental Geochemistry (SKLEG2018907). The views expressed in this article are those of the authors and do not necessarily reflect the views or policies of the US Environmental Protection Agency.

References

Ahmad M, Rajapaksha AU, Lim JE, Zhang M, Bolan N, Mohan D, Vithanage M, Lee SS, Ok YS (2014) Biochar as a sorbent for contaminant management in soil and water: a review. Chemosphere 99:19–33

Ai L, Zhang C, Liao F, Wang Y, Li M, Meng L, Jiang J (2011) Removal of methylene blue from aqueous solution with magnetite loaded multiwall carbon nanotube: kinetic, isotherm and mechanism analysis. J Hazard Mater 198:282–290

Almeida C, Debacher N, Downs A, Cottet L, Mello C (2009) Removal of methylene blue from colored effluents by adsorption on montmorillonite clay. J Colloid Interface Sci 332:46–53

Benhouria A, Islam MA, Zaghouane-Boudiaf H, Boutahala M, Hameed BH (2015) Calcium alginate–bentonite–activated carbon composite beads as highly effective adsorbent for methylene blue. Chem Eng J 270:621–630

Bulut Y, Aydın H (2006) A kinetics and thermodynamics study of methylene blue adsorption on wheat shells. Desalination 194:259–267

Ding ZH, Wan YS, Hu X, Wang SS, Zimmerman AR, Gao B (2016) Sorption of lead and methylene blue onto hickory biochars from different pyrolysis temperatures: importance of physicochemical properties. J Ind Eng Chem 37:261–267

Doğan M, Alkan M, Türkyilmaz A, Özdemir Y (2004) Kinetics and mechanism of removal of methylene blue by adsorption onto perlite. J Hazard Mater 109:141–148

Fang J, Gao B, Zimmerman AR, Ro KS, Chen JJ (2016) Physically (CO_2) activated hydrochars from hickory and peanut hull: preparation, characterization, and sorption of methylene blue, lead, copper, and cadmium. RSC Adv 6:24906–24911

Foo KY, Hameed BH (2010) Insights into the modeling of adsorption isotherm systems. Chem Eng J 156:2–10

Gong J-L, Wang B, Zeng G-M, Yang C-P, Niu C-G, Niu Q-Y, Zhou W-J, Liang Y (2009) Removal of cationic dyes from aqueous solution using magnetic multi-wall carbon nanotube nanocomposite as adsorbent. J Hazard Mater 164:1517–1522

Gotoh T, Matsushima K, Kikuchi K-I (2004) Preparation of alginate–chitosan hybrid gel beads and adsorption of divalent metal ions. Chemosphere 55:135–140

Gupta VK, Suhas AI, Saini VK (2004) Removal of rhodamine B, fast green, and methylene blue from wastewater using red mud, an aluminum industry waste. Ind Eng Chem Res 43:1740–1747

Gupta VK, Kumar R, Nayak A, Saleh TA, Barakat MA (2013) Adsorptive removal of dyes from aqueous solution onto carbon nanotubes: a review. Adv Colloid Interf Sci 193-194:24–34

Hameed BH, Din ATM, Ahmad AL (2007) Adsorption of methylene blue onto bamboo-based activated carbon: kinetics and equilibrium studies. J Hazard Mater 141:819–825

Hassan A, Abdel-Mohsen A, Fouda MM (2014) Comparative study of calcium alginate, activated carbon, and their composite beads on methylene blue adsorption. Carbohydr Polym 102:192–198

Helland A, Wick P, Koehler A, Schmid K, Som C (2008) Reviewing the environmental and human health knowledge base of carbon nanotubes. Ciênc Saúde Coletiva 13:441–452

Hoet PH, Brüske-Hohlfeld I, Salata OV (2004) Nanoparticles—known and unknown health risks. J Nanobiotechnol 2:12

Inyang MI, Gao B, Yao Y, Xue YW, Zimmerman A, Mosa A, Pullammanappallil P, Ok YS, Cao XD (2016) A review of biochar as a low-cost adsorbent for aqueous heavy metal removal. Crit Rev Env Sci Tec 46:406–433

Kulkarni AR, Soppimath KS, Aminabhavi TM, Dave AM, Mehta MH (2000) Glutaraldehyde crosslinked sodium alginate beads containing liquid pesticide for soil application. J Control Release 63:97–105

Lam C-W, James JT, McCluskey R, Arepalli S, Hunter RL (2006) A review of carbon nanotube toxicity and assessment of potential occupational and environmental health risks. Crit Rev Toxicol 36:189–217

Lee KY, Mooney DJ (2012) Alginate: properties and biomedical applications. Prog Polym Sci 37:106–126

Li Y-H, Di Z, Ding J, Wu D, Luan Z, Zhu Y (2005) Adsorption thermodynamic, kinetic and desorption studies of Pb^{2+} on carbon nanotubes. Water Res 39:605–609

Li Y, Du Q, Liu T, Sun J, Wang Y, Wu S, Wang Z, Xia Y, Xia L (2013) Methylene blue adsorption on graphene oxide/calcium alginate composites. Carbohydr Polym 95:501–507

Limousin G, Gaudet J-P, Charlet L, Szenknect S, Barthes V, Krimissa M (2007) Sorption isotherms: a review on physical bases, modeling and measurement. Appl Geochem 22:249–275

Lin Y-B, Fugetsu B, Terui N, Tanaka S (2005) Removal of organic compounds by alginate gel beads with entrapped activated carbon. J Hazard Mater 120:237–241

Liu L, Wan Y, Xie Y, Zhai R, Zhang B, Liu J (2012) The removal of dye from aqueous solution using alginate-halloysite nanotube beads. Chem Eng J 187:210–216

Lyu H, Gao B, He F, Ding C, Tang J, Crittenden JC (2017) Ball-milled carbon nanomaterials for energy and environmental applications. ACS Sustain Chem Eng 5:9568–9585

Lyu H, Gao B, He F, Zimmerman A, Ding C, Huang H, Tang J (2018a) Effects of ball milling on the physicochemical and sorptive properties of biochar: experimental observations and governing mechanisms. Environ Pollut 233:54–63

Lyu H, Gao B, He F, Zimmerman A, Ding C, Huang H, Tang J, Crittenden J (2018b) Experimental and modeling investigations of ball-milled biochar for the removal of aqueous methylene blue. Chem Eng J 335:110–119

Mahmoodi NM (2011) Equilibrium, kinetics, and thermodynamics of dye removal using alginate in binary systems. J Chem Eng Data 56: 2802–2811

Manna S, Roy D, Saha P, Gopakumar D, Thomas S (2017) Rapid methylene blue adsorption using modified lignocellulosic materials. Process Saf Environ Prot 107:346–356

Park HG, Kim KH, Chae MY, Oh EG, Lee EY (2006) Alginate gel based adsorbents for heavy metal removal. Samsung General Chemicals Co., Ltd

Patra S, Roy E, Madhuri R, Sharma PK (2016) Agar based bimetallic nanoparticles as high-performance renewable adsorbent for removal and degradation of cationic organic dyes. J Ind Eng Chem 33:226–238

Peterson SC, Jackson MA, Kim S, Palmquist DE (2012) Increasing biochar surface area: optimization of ball milling parameters. Powder Technol 228:115–120

Peydayesh M, Rahbar-Kelishami A (2015) Adsorption of methylene blue onto Platanus orientalis leaf powder: kinetic, equilibrium and thermodynamic studies. J Ind Eng Chem 21:1014–1019

Rajapaksha AU, Chen SS, Tsang DCW, Zhang M, Vithanage M, Mandal S, Gao B, Bolan NS, Ok YS (2016) Engineered/designer biochar for contaminant removal/immobilization from soil and water: potential and implication of biochar modification. Chemosphere 148:276–291

Rocher V, Bee A, Siaugue J-M, Cabuil V (2010) Dye removal from aqueous solution by magnetic alginate beads crosslinked with epichlorohydrin. J Hazard Mater 178:434–439

Sarkar S, SenGupta AK, Prakash P (2010) The Donnan membrane principle: opportunities for sustainable engineered processes and materials. Environ Sci Technol 44:1161–1166

Wang S, Li L, Wu H, Zhu ZH (2005) Unburned carbon as a low-cost adsorbent for treatment of methylene blue-containing wastewater. J Colloid Interface Sci 292:336–343

Wang B, Gao B, Fang J (2017) Recent advances in engineered biochar productions and applications. Crit Rev Environ Sci Technol 47: 2158–2207

Xu XB, Hu X, Ding ZH, Chen YJ, Gao B (2017) Waste-art-paper biochar as an effective sorbent for recovery of aqueous Pb(II) into value-added PbO nanoparticles. Chem Eng J 308:863–871

Yagub MT, Sen TK, Afroze S, Ang HM (2014) Dye and its removal from aqueous solution by adsorption: a review. Adv Colloid Interf Sci 209:172–184

Yao Y, Xu F, Chen M, Xu Z, Zhu Z (2010) Adsorption behavior of methylene blue on carbon nanotubes. Bioresour Technol 101: 3040–3046

Zhang M, Gao B (2013) Removal of arsenic, methylene blue, and phosphate by biochar/AlOOH nanocomposite. Chem Eng J 226:286–292

Zohre S, Ataallah SG, Mehdi A (2010) Experimental study of methylene blue adsorption from aqueous solutions onto carbon nano tubes. Int J Water Resour Environ Eng 2:016–028